Progress in PHOTOVOLTAICS

PROGRESS IN PHOTOVOLTAICS: RESEARCH AND APPLICATIONS
Prog. Photovolt: Res. Appl. 2012; **20**:954–959
Published online 25 July 2011 in Wiley Online Library (wileyonlinelibrary.com). DOI: 10.1002/pip.1156

SHORT COMMUNICATION

Limiting photovoltaic efficiency under new ASTM International G173-based reference spectra

Martin A. Green*

ARC Photovoltaics Centre of Excellence, University of New South Wales (UNSW), Sydney 2052, Australia

ABSTRACT

Efficiency limits upon photovoltaic energy conversion are re-evaluated under the new ASTM International G173-based reference spectra. Peak terrestrial efficiency for a single-junction device increases to 33.8% under the new air mass 1.5G spectrum, whereas overall and time-symmetric limits increase to 74.0% and 68.0%, respectively. Copyright © 2011 John Wiley & Sons, Ltd.

KEYWORDS

efficiency limits; solar reference spectra; Shockley–Queisser limits

***Correspondence**

Martin A. Green, ARC Photovoltaics Centre of Excellence, University of New South Wales (UNSW), Sydney 2052, Australia.
E-mail: m.green@unsw.edu.au

Received 10 December 2010; Revised 21 March 2011

1. INTRODUCTION

In April 2008, the global reference spectrum tabulated in international standard International Electrotechnical Commission (IEC) 60904-3 was revised to Edition 2 to become IEC 60904-3 Ed. 2: 2008 [1]. The new global spectrum is identical to that tabulated in ASTM International G173-03, which also tabulates a direct normal spectrum, with both deduced from a tabulated air mass zero (AM0) spectrum. It is likely that the ASTM G173-03 direct normal spectrum (which includes 5.8° of circumsolar radiation) will also become an international standard. Progress in Photovoltaics commenced reporting record experimental solar cell efficiency results referenced to the new spectra from January 2009 [2].

The tabulated spectra for extraterrestrial AM0 and for global and direct normal (energy density) AM1.5 conditions are shown in Figure 1(a) over the 0.28–4.0-μm wavelength range for which the spectra are tabulated. Following Planck [3], a temperature can be defined that describes the intensity at each wavelength equal to that of a blackbody that would emit radiation of the same intensity at that wavelength (making this temperature wavelength dependent for any radiation other than blackbody radiation). These temperatures have thermodynamic connotations as subsequently exploited.

The uppermost three curves in Figure 1(b) show the Planckian equivalent temperature, T_e, if the entire spectral intensity of the three energy spectra is considered confined to the solid angle subtended by the solar disc, whereas the lowermost curves show the corresponding temperatures if the radiation is 'diluted' [4] by spreading over the whole sky (dilution by 46200 times [5]). The uppermost set is relevant to systems converting only the direct component of sunlight whereas the lowermost set is relevant to devices that convert sunlight equally well from any angle in the sky.

Interestingly, in the diluted radiation case, the Planckian equivalent temperature can approach and even fall below the cell temperature, taken as 25°C (298.15K) for photovoltaic measurements. To nullify the 'second quadrant' energy conversion effectively using the cooler sky as a sink at such wavelengths as opposed to the normal 'fourth quadrant' operation, the converter response was limited to a maximum of 4-μm wavelength.

2. LANDSBERG LIMIT

The Landsberg limit [4] represents an upper bound on the possible efficiency of conversion of solar energy to electricity (or other useful work) but can only be attained in a system where normal time symmetry is avoided by the

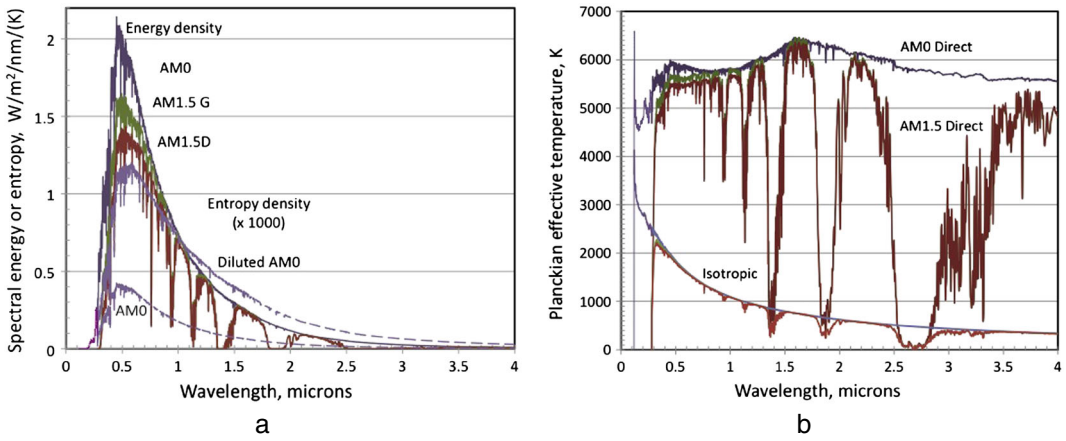

Figure 1. (a) Energy spectral density for the new reference spectra (entropy spectral density is also shown on an enlarged scale in the lower section of the graph as dashed lines for the diluted and direct AM0 spectrum); (b) Planckian equivalent temperature versus wavelength for the three spectra.

use of non-reciprocal elements such as optical circulators [5,6]. With reference to the energy and entropy fluxes of Figure 2, the generalised form of the Landsberg limit is as follows:

$$\eta_L = \left(1 - T_A \dot{S}_S/\dot{E}_S\right) - \left(1 - T_A \dot{S}_C/\dot{E}_C\right)\dot{E}_C/\dot{E}_S \qquad (1)$$

$\dot{E}_C$ in the Landsberg limit is the energy emitted by a blackbody at ambient temperature so both this and $\dot{S}_C$ can be calculated analytically [5]. $\dot{E}_S{}^S$ can be found by integration of the tabulated spectral density data $\dot{E}_{\lambda S}$. $\dot{S}_S{}^S$ can be calculated using Planck's equivalent temperature approach by calculating the entropy spectral density from the energy spectral density (assuming unpolarised light) as follows [3,7]:

$$\dot{S}_{\lambda S} = \frac{2\pi k c f_c}{\lambda^4}[(1+a)\ln(1+a) - a\ln a] \qquad (2)$$

$$\text{where } a = \frac{\lambda^5 \dot{E}_{\lambda S}}{2\pi f_c h c^2}$$

where f_c is unity if light is considered uniformly distributed over the sky and much smaller (1/46200) if confined to the angle subtended by the sun's disc.

Results obtained by integrating spectral components calculated in this way are shown in Table I. For the two terrestrial AM1.5 spectra, the energy content was assumed zero beyond 4 μm wavelength, whereas the AM0 spectrum was extended to both shorter and longer wavelength using values from a related tabulation [8], although the converter response was also limited to 4 μm for diluted AM0 radiation.

Note that 'dilution' of the radiation by considering it uniformly distributed over the hemisphere rather than coming entirely from the sun's disc increases the entropy content by 4.03 for the AM0 spectrum and by 3.68 and 3.69 for the AM1.5G and AM1.5D spectra, respectively. From Equation (1), once $\dot{E}_{\lambda S}/\dot{S}_{\lambda S}$ becomes less than T_A, the Landsberg efficiency for conversion of the AM0 spectrum will tend to decrease if the spectral response is extended to longer wavelengths. For the 'diluted' AM0 spectrum, this condition occurs at a wavelength of 4.08 μm.

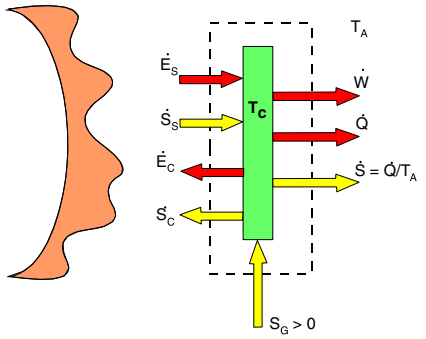

Figure 2. Entropy and energy fluxes involved in calculating the Landsberg limit.

Table I. Landsberg efficiency parameters for the three ASTM G173-03 spectra in the case of direct and global light converters.

	AM0		AM1.5G		AM1.5D	
Parameter	Direct	Global	Direct*	Global	Direct	Global*
$\dot{E}_S$ (W/m^2)	1366.1		1000.4		900.1	
$\dot{S}_S$ (W/m^2/k)	0.3148	1.270	0.2373	0.8722	0.2188	0.8068
η_L (%)	93.1	72.6	92.9	74.0	92.8	73.3

Tabulated AM0 spectrum extended to both shorter and longer wavelength; AM1.5 spectrum terminated at 4-μm wavelength; T_A=25°C. Values are those obtained by trapezoidal integration of the tabulated data and of those calculated from these data.

*Included for reference.

To avoid issues that consequently arise, it was assumed the converter does not respond to wavelengths longer than 4μm in this case as well.

3. TRIVICH–FLINN LIMIT

The early analysis by Trivich and Flinn [9] of the bandgap dependence of efficiency for a simple, single energy threshold, photovoltaic converter essentially analysed the absorption part of the process. The analysis considered the ratio between the energy of photogenerated electron–hole pairs separated by the bandgap energy E_g and the total energy of incident sunlight, defining the efficiency of this conversion as follows:

$$\eta_{TF} = E_g \int_{E_g}^{\infty} \dot{N}_S dE \Big/ \int_{0}^{\infty} \dot{E}_S dE \tag{3}$$

where $\dot{E}_S$ is the energy flux and $\dot{N}_S$ is the particle flux ($\dot{N}_S = \dot{E}_S/E$ where $E=hf$ is the photon energy).

The Trivich–Flinn (TF) limit would apply to the overall conversion process if all the photogenerated carriers could be extracted at close to the 'bandgap voltage' E_g/q. It is shown subsequently that this is possible in principle for low bandgap cells operating under high intensity. The efficiency of devices near local extrema is also thermodynamically related to the TF efficiency, of interest for these reasons, although always representing an upper bound on attainable efficiency for a simple, single threshold device.

4. SHOCKLEY–QUEISSER LIMIT [10]

Generalised to the chemical potential model of photon emission, the Shockley–Queisser (SQ) equation for the power density output of a solar cell with a single energy absorption threshold is given by

$$JV = qV\left(\int_{E_g}^{\infty} \dot{N}S dE - \frac{2\pi}{h^3c^2}\int_{E_g}^{\infty} \frac{E^2 dE}{\exp[(E-qV)/kT_A]-1}\right) \tag{4}$$

where $\dot{N}_S$ can be expressed as

$$\dot{N}_S = \frac{2\pi}{h^3c^2}\left(\int_{E_g}^{\infty} \frac{E^2 dE}{\exp[E/kT_e(E)]-1}\right) \tag{5}$$

The first term in the brackets of Equation (4) corresponds to the integrated photon flux in sunlight of energy above the bandgap. Partial differentiation of Equation (4) gives [11]

$$\frac{\partial(JV)}{\partial E_g} = \frac{2\pi qV}{h^3c^2}\left(\frac{{E_g}^2}{\exp\left[E_g/kT_e(E_g)\right]-1} - \frac{{E_g}^2}{\exp\left[(E_g-qV)/kT_A\right]-1}\right) \tag{6}$$

A necessary condition for a stationary point to occur in a plot of η versus E_g is that Equation (6) is zero, giving a corresponding voltage V_{cv} that will be referred to as the 'Carnot voltage' for obvious reasons [11]:

$$V_{CV} = E_g\left[1 - T_A/T_e(E_g)\right]/q \tag{7}$$

Evaluating Equation (4) using this voltage will result in a power output that will always be less than or equal to the maximum possible, with equality only obtained for those values of E_g giving a stationary point in the generalised SQ efficiency as a function of E_g.

The second integral in Equation (4) is in the form of a very general Bose–Einstein integral [4] with these integrals closely related to polylogarithms $Li_s[z]$ defined as [12]

$$Li_s[z] = \sum_{k=1}^{\infty} z^k/k^s \tag{8}$$

The second integral in Equation (4) can be evaluated as [5]

$$\int_{E_g}^{\infty} \frac{E^2 dE}{\exp\left[(E-qV)/kT_A\right]-1} = E_g^2(kT_A)Li_1\left[\exp\left\{\left(qV-E_g\right)/kT_A\right\}\right] + 2E_g(kT_A)^2Li_2\left[\exp\left\{\left(qV-E_g\right)/kT_A\right\}\right] + 2(kT_A)^3Li_3\left[\exp\left\{\left(qV-E_g\right)/kT_A\right\}\right] \tag{9}$$

Note that for small arguments such as when $V<<E_g/q$, the polylogarithm values approach those of their arguments ($Li_s[z]\rightarrow z$ as $z\rightarrow 0$), so the expression simplifies down to

$$\int_{E_g}^{\infty} \frac{E^2 dE}{\exp[(E-qV)/kT_A]-1} = 2(kT_A)^3\left[\left(E_g/kT_A\right)^2/2 + E_g/kT_A + 1\right]\exp\left[\left(qV-E_g\right)/kT_A\right] \tag{10}$$

The formulation then corresponds to the original SQ approach and also to 'ideal diode' behaviour. However, because $Li_1(z) = -\ln(1-z)$ approaches infinity as its argument approaches unity, the more general formulation of Equation (9) shows the open-circuit voltage of a perfectly absorbing solar cell can never exceed its bandgap, no matter how intense the illumination (thin cells can however, in principle [4,13]).

The difference between the two formulations becomes most apparent for small bandgap cells at high concentration (or small angular confinement). Figure 3 shows the normalised current–voltage curves for cells in the bandgap range of 0.4–1.0 eV under the maximal intensity conditions for the AM1.5D spectrum. For these bandgaps (and for higher bandgaps up to 1.58 eV), the original SQ formulation is problematic in that it predicts an open-circuit voltage higher than the bandgap voltage, when the formulation would no longer be self-consistent. However, the formulation remains accurate for voltages below the bandgap voltage. It is only when the maximum powerpoint calculated by the SQ approach approaches the bandgap that any appreciable error in calculated efficiency will occur.

5. SINGLE CELL LIMIT

Efficiency versus bandgap computed for the different spectra in the extended SQ approach are summarised in Figure 4. The uppermost curve is the Trivich–Flinn limit for the AM1.5D spectrum, which is approached for small bandgap cells under high concentration levels (or severe angular restriction of cell response). Note that the limiting efficiency under concentration (or angular restriction) increases more rapidly for small bandgap cells than for large bandgap cells (the approximately 60-mV increase in open-circuit voltage for 10 times increase in intensity, or decrease in angular acceptance, is proportionately larger for small bandgap cells).

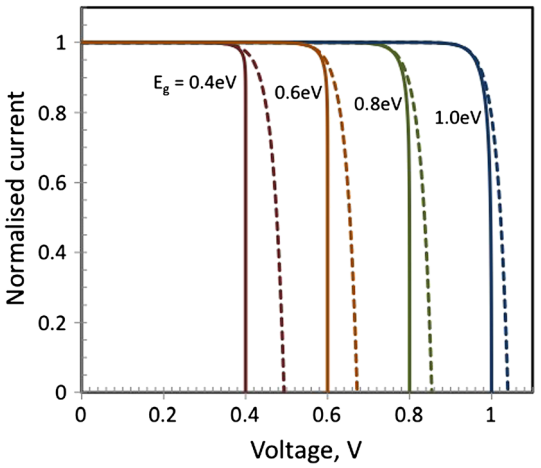

Figure 3. Current–voltage curves for cells of the bandgaps indicated under maximal concentration or maximal angular restriction. The dashed curves show the result of the original Shockley–Queisser formulation, whereas the solid lines show the results of the more complete chemical potential formulation.

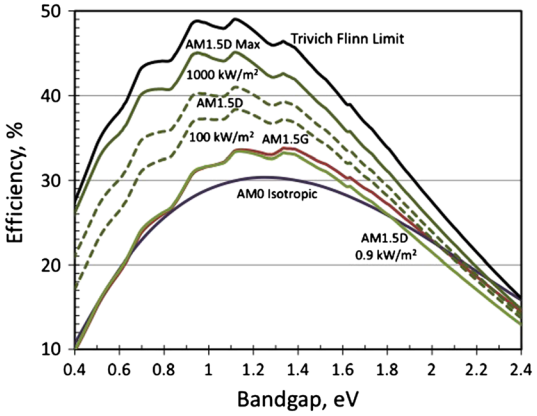

Figure 4. Isotropic performance limits for cells under the AM0, AM1.5 and AM1.5D spectral, as well as for the AM1.5D spectra under various concentration levels. The Trivich–Flinn limit for the AM1.5D spectrum is shown for comparison.

For the AM0 spectrum for a cell with isotropic response, there is a single peak (30.4% efficiency for E_c = 1.245 eV). For the terrestrial AM1.5 spectra, there are multiple peaks because of the strong water vapour absorption bands apparent in Figure 1(a). The most important are the absorption bands in the 920–970 nm (1.28–1.35 eV), 1100–1160 nm (1.07–1.13 eV) and 1300–1500 nm (0.83–0.95 eV) wavelength (energy) ranges.

Loss of radiation in the terrestrial spectra due to the first of these bands wipes out the 'natural' peak apparent in the AM0 spectrum, creating minimum and maxima on either side of the absorption band. A local maximum occurs on the high energy side of the absorption band, with a local minimum on the low energy side.

Note that from Figure 4, the AM0 and AM1.5G spectra give higher efficiency for large bandgap than for the AM1.5D spectra. This is due to blue photons being selectively scattered out of the AM1.5D spectrum during passage through the atmosphere. This, combined with the intensity dependence already noted, shifts the global maximum between three different peaks, each associated with the high energy side of the three absorption bands already mentioned.

6. AM1.5G ISOTROPIC LIMITS AND EXPERIMENTAL DATA

The solid line of Figure 5 again shows the limiting efficiency for a conventional cell with isotropic response under the new AM1.5G spectrum. The stronger spectral content over the 650–900 nm range, compared with the previous standard, shifts the peak efficiency to higher energy so that the two peaks around 1.15 eV and 1.35 eV are nearly equal, with peak efficiencies of 33.6% and

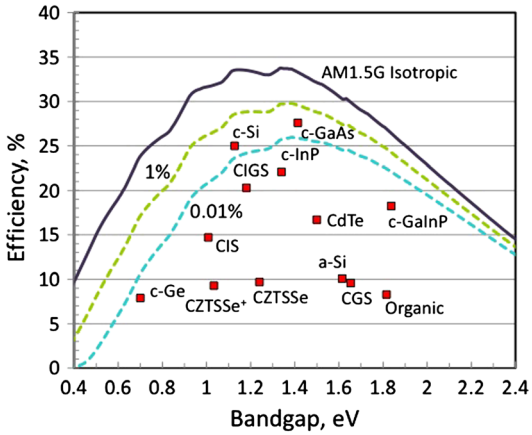

Figure 5. Isotropic efficiency limits under the AM1.5G spectrum and also for devices with 1% and 0.01% radiative efficiency. Also shown are best certified cell limits efficiencies for various cell technologies.

33.8%, respectively. For the previous reference spectrum (ASTM E892-87, IEC 60904-3:1989), the order of the peaks was reversed and both were about 1% (relative) lower in efficiency [14], consistent with expectations discussed elsewhere [2].

Also shown as dashed lines are the limiting efficiencies for 1% and 0.01% radiative efficiencies of the cell, with radiative efficiency defined as the fraction of net recombination in the device that is radiative (with this definition, radiative recombination currents are multiplied by 100 and 10000 for 1% and 0.01% radiative efficiency, respectively). The radiative efficiency is a measure of the state of development of the cell material technology. Limiting efficiencies calculated are identical to those calculated under a reduced intensity (further dilution) of sunlight. Hence, the previous curves under concentration (Figure 4) can also be used to calculate the effects of non-ideal radiative efficiency in this case as well (for example, the curve for 100-kW/m^2 incident intensity represents the limiting performance for a cell under 1000-kW/m^2 intensity, if the radiative efficiency is 10% rather than 100%).

Given this correspondence, it is not surprising that the efficiency for low bandgap cells is most sensitive to low values of the radiative efficiency, because a 60 mV/decade voltage reduction with decreasing radiative efficiency has a proportionately more devastating impact. Peak efficiency is pushed to higher bandgap cells as the radiative efficiency decreases.

Also shown in Figure 5 are best certified experimental values for a range of different solar cell technologies [15]. 'Bandgap' corresponds to the energy on the low energy side of the spectral response curve where external quantum efficiency reaches 50% of its peak value. Silicon (c-Si) and c-GaAs lie above the 0.01% radiative efficiency line. Actual radiative efficiencies are close to or above 1% for both technologies, because experimental devices have additional losses other than the radiative loss assumed (including, for example, reflection and resistance losses and also including additional radiative loss due to non-abrupt absorption thresholds [16]). Relatively low radiative efficiency for GaAs devices can be due to the large amount of radiative emission from the active region into the substrate where most is absorbed.

7. MULTIJUNCTION CELLS

Cell efficiency can be improved by using cells of different bandgap to convert different parts of the spectrum. The limit for an infinite number of cells provides not only an upper bound on the performance gains possible by this approach but also a thermodynamic limit on photovoltaic conversion efficiency for any time-symmetric photovoltaic system. In this case, there is no energy loss on absorption and also isoentropic carrier collection.

For the infinite cell limit, where the emission from any cell can be considered to be restricted to a single energy by low pass energy filters [17], the current density from each cell is given by [5]

$$dJ = \frac{2\pi q f_c}{h^3 c^2}\left(\frac{E_g^2}{\exp\left[\left(E_g/T_e(E_g)\right]-1}-\frac{E_g^2}{\exp\left[\left(E_g-qV\right)/kT_A\right]-1}\right)dE_g \quad (14)$$

Note that this current becomes zero at the 'Carnot voltage', showing that the Carnot voltage corresponds to

Table II. Summary of photovoltaic efficiency limits under the three ASTM G173-03 spectra.

	AM0		AM1.5G		AM1.5D	
Efficiency	Direct	Isotropic	Direct*	Isotropic	Direct	Isotropic*
Landsberg (ultimate)	93.1	72.6	92.9	74.0	92.8	73.3
Time symmetric (infinite tandem)	86.3	66.6	86.4	68.0	86.0	67.2
Single cell (bandgap)	40.7 (1.006eV)	30.4 (1.245eV)	45.2 (1.119eV)	33.8 (1.339eV)	45.1 (1.117eV)	33.4 (1.135eV)

*Included for reference.

the open-circuit voltage in this case [11]. Maximum power is obtained by backing off from this voltage as in a normal cell, with the maximum powerpoint voltage for each bandgap given implicitly by

$$V_{mp} = E_g(1 - T_A/T_e)/q - (kT_A/q)\ln\left\{\frac{1 + (qV_{mp}/kT_A) - \exp[(qV_{mp} - E_g)/kT_A]}{1 + [(qV_{mp}/kT_A) - 1]\exp[(qV_{mp} - E_g)/kT_A]}\right\} \quad (15)$$

Optimising the power output for each incremental energy range by finding the optimal voltage allows the energy contribution from each cell to be found and hence the overall energy conversion efficiency. The time-symmetric limits follow the same trends as the time asymmetric Landsberg limits with values 92–93% of the latter.

Operating the ideal multijunction cells at close to the open-circuit voltage point would allow the Carnot efficiency to be approached, if the light emitted back to the sun were not treated as a loss. The only additional loss arises from having to move away from this operating point to improve the balance between the power extracted and that sent back to the sun. In a time asymmetric system, the latter can be minimised by removing symmetry between emission and absorption properties.

A summary of the various efficiencies discussed is shown in Table II.

REFERENCES

1. International Standard, IEC 60904–3, Edition 2, 2008, Photovoltaic Devices—Part 3: Measurement Principles for Terrestrial Photovoltaic (PV) Solar Devices with Reference Spectral Irradiance Data. ISBN 2–8318–9705-X, *International Electrotechnical Commission*, April 2008.
2. Green MA, Emery K, Hishikawa Y, Warta W. Solar cell efficiency tables (Version 33). *Progress in Photovoltaics* 2009; **17**: 85–94.
3. Planck M. The Theory of Heat Radiation. *Dover: New York*, 1959 [English translation of Planck M. Vorlesungen über die Theorie der Warmestrahlung. *Leipzig: Barth*, 1913].
4. Landsberg PT, Tonge G. Thermodynamic energy conversion efficiencies. *Journal of Applied Physics* 1980; **51**: R1–R20.
5. Green MA. Third Generation Photovoltaics: Advanced Solar Energy Conversion. Springer-Verlag: Berlin, 2003.
6. Ries H. Complete and reversible absorption of radiation. *Applied Physics* 1983; **B32**: 153.
7. Kabelac S, Drake FD. The entropy of terrestrial solar radiation. *Solar Energy* 1992; **48**: 239–248.
8. ASTM Standard Extraterrestrial Spectrum Reference E-490-00 2006 (tabulated at http://rredc.nrel.gov/solar/spectra/am0/).
9. Trivich D, Flinn PA. Maximum efficiency of solar energy conversion by quantum processes. In: *Solar Energy Research,* Daniels F, Duffie J (eds). Thames and Hudson: London, 1955.
10. Shockley W, Queisser HJ. Detailed balance limit of efficiency of p-n junction solar cells. *Journal of Applied Physics* 1961; **32**: 510–519.
11. Landsberg P. Efficiencies of solar cells: Where is Carnot hiding? Conference Record, *16th European Photovoltaic Solar Energy Conference*; Glasgow, 2000.
12. Lewin L Polylogarithms and Associated Functions. North-Holland: New York, 1981 (also see http://en.wikipedia.org/wiki/Polylogarithm).
13. Parrott JE. Self-consistent detailed balance treatment of the solar cell. *IEEE Proceedings* 1986; **133**: 314–318.
14. Tiedje T, Yablonowitch E, Cody GD, Brooks, BG. Limiting efficiency of silicon solar cells. *IEEE Transactions on Electron Devices* 1984; **ED-31**: 711–716.
15. Green MA, Emery K, Hishikawa Y, Warta W. Solar cell efficiency tables (Version 37). *Progress in Photovoltaics* 2011; **19**: 84–92.
16. Kirchartz T, Taretto K, Rau U. Efficiency limits of organic bulk heterojunction solar cells. *Journal of Physical Chemistry C* 2009; **113**: 17958–17966.
17. Marti A, Araujo GL. Limiting efficiencies for photovoltaic energy conversion in multigap systems. *Solar Energy Materials and Solar Cells* 1996; **43**: 203–222.